Temperature-Induced Water Release and Uptake in Organic Porous Networks

Natalia Pérez-Hernández,*,† Eduardo H. L. Falcao,‡ Cirilo Pérez,§ Diego Fort,† Julio D. Martín,† and Juergen Eckert*,‡

Instituto de Investigaciones Químicas, Avda. Américo Vespucio, 49, 41092 Seville, Spain, Materials Research Laboratory, University of California, Santa Barbara, California 93106, and Instituto de Bioorgánica, Universidad de La Laguna, CSIC, Ctra. Vieja de La Esperanza 2, 38206 La Laguna, Tenerife, Spain

Received: December 17, 2009; Revised Manuscript Received: March 24, 2010

The behavior of water confined near nonpolar surfaces has important implications for a number of biological phenomena. In this type of confined environment the properties of "hydrophobicity" and "hydrophilicity" are closely related to the structure of the interfacial water, which in turn can depend on temperature in a very subtle way. Although the physical-chemical consequences of this fact have been theoretically addressed to a great extent, the underlying thermodynamic question is still widely discussed. Accordingly we performed thermogravimetric analysis and variable-temperature powder X-ray diffraction studies on representative hydrogen bonding organic pores occupied by water. The results indicate that a hydrophilic-to-hydrophobic transition of the inner surface of the pores occurs upon increasing temperature, which may be attributed to a strong influence of the dynamics and thermodynamics of local water molecules on the surface affinity of the pores. The relevance of our findings to the understanding of the phenomenon of water transport in natural pores is discussed.

Introduction

The transport of water through natural membrane channels is a phenomenon of considerable biological importance. However, a detailed understanding of the driving forces for filling of the predominantly "hydrophobic" natural pores with water and of the attendant functional thermodynamics remains elusive.[1] Hydrophobic does not in this context mean "water-repellent" but rather implies that the attraction at the interface between water and the inner surface of the pore is less than that between water molecules. To fully understand this phenomenon it is necessary to know both the equilibrium structures and the particular behavior of the transient local structures of the entrapped water on a molecular scale.[2−4]

The structure of water in natural channels has been studied by using molecular dynamics simulations;[5] biological systems, however, are characterized by numerous chemical and structural complexities, which makes it necessary to evaluate model systems of much greater simplicity. These models are in general chosen to only address some particular features of the system under study. Nonetheless, results obtained for different model systems strongly suggest that there is a considerable degree of universality with regard to the behavior of entrapped water.[6−8] For example, single-walled carbon nanotubes have been demonstrated to be the simplest model system specifically valid for modeling entrapped water in biological structures, such as in aquaporin water channels[9−13] and other important nanofluidic systems.[14−17] An important limitation, however, of the application of such nanoporous media to the study of the structure and dynamics of long-lived aggregates of water molecules is that it is not always possible to support mechanisms determined *in silico* with those derived from specific experiments.[18−23] For example, one of the most important predictions obtained from room temperature molecular dynamics simulation studies is that the structure and dynamics of water are specific to each model and depend on the inner diameter[24−27] and sometimes also on the hydrophilicity[28,29] of the pore. Yet, experimental evidence to support this conclusion is lacking and a rigorous understanding of the mechanisms of water transport and conduction through pores remains incomplete. A sophisticated understanding of these processes requires that computational studies be complemented by experimental data.[30] Our central concern has been to establish and utilize models of pores which reflect biologically relevant chemical principles whereby we could facilitate an explicit experimental verification of simulated data.[31−35]

In this paper we utilize parallel thermogravimetric analysis (TGA) and variable-temperature powder X-ray diffraction (VT-PXRD) to show that in our model systems of water pores the observed freely moving water clusters[36] are stable at or below room temperature but unstable at higher temperatures and reach a point at which they are able to leave the pore. This result implies that the inner pore surface switches from hydrophilic to hydrophobic, which represents an experimental confirmation that the near coexistence between water-filled and water-empty states of the pore and the sensitivity to small temperature perturbations are functionally relevant.[37] We will also discuss the implications of these experimental findings for the functioning of natural systems.

Background and Objectives

We designed suitable solid state porous organic assemblies formed by monomers **1** and **2** (Figure 1) as chemical models to elucidate specific mechanisms of water transport. The non-uniform van der Waals diameter exhibits a range from 5.9 to 9.4 Å in pores formed by monomers of chemical structure **1** and from 4.2 to 6.5 Å in pores formed by monomers of chemical structure **2** (see Figure 1, inset)[36] depending on the size of the side chains of the organic molecules used to construct the pore.

* To whom correspondence should be addressed. E-mail: natalia.perez@iiq.csic.es (N.P.-H.) and juergen.eckert@mrl.ucsb.edu (J.E.).
† Instituto de Investigaciones Químicas.
‡ University of California.
§ Instituto de Bioorgánica, Universidad de La Laguna.

10.1021/jp911930k
Published on Web 04/09/2010

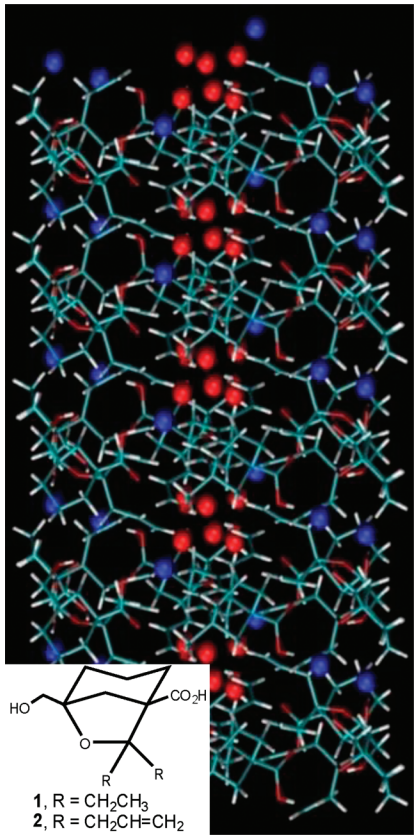

Figure 1. A side view of the open pore formed by (±)**2**·2H_2O.[37] The organic molecule is in capped-stick representation, water molecules are represented by spheres: structural water, blue; cluster, red. Inset: Chemical structures for monomers **1** and **2**, the hydroxyl/acids that form hydrated pores by crystallization from wet carbon tetrachloride.[31,36]

In both model systems the proportion of water in the pores is the same and water molecules can be taken up and released over a wide range of temperatures without impairing the structure of hydrogen-bonded networks. Furthermore, these pores should be just wide enough at their narrowest region for water molecules to pass through, which in turn provides size selectivity while imposing single-file water diffusion.

Experimental evidence of water occupancy of nonpolar cavities in thermodynamic equilibrium has previously been reported.[38,39] In our models, we find two apparently different types of water molecules: on the one side, water located at the surface of the pore remains mainly in the H-bonding pattern from which the structure is built up, and on the other hand, water molecules in clusters distributed along the pore (similar in topology to liquid and gas-phase flickering cluster models detected by spectroscopy[40−47]), which produce a wetting path that explains the observed permeability[36] (Figure 1). The dynamics of pores occupied by water molecules can be described on the basis of the hydrophobic effect,[48] which is known to be temperature dependent.[49] Our previous work demonstrated that water could fluctuate between being vapor-like in the empty state of the pore and liquid-like in the filled state (Figure 2) at saturated vapor pressure and at temperatures of 25 °C and below.[36]

Our objective is to describe the effect of temperature on the nature of the inner surface (hydrophobic or hydrophilic) of our pores on the basis of our experiments, and this way understand better how this affects the thermodynamic function in natural pores and the influence of water in the stability of the assemblies. This type of evidence for such an effect has proven difficult to

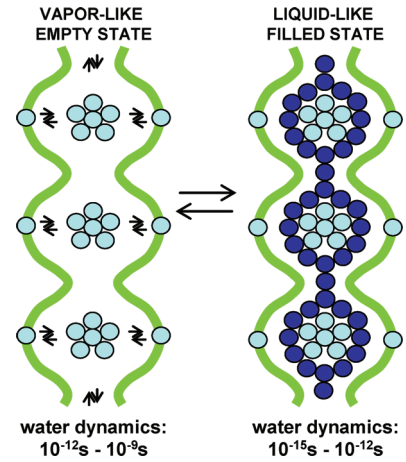

Figure 2. Two-state-like behavior of our models of water pores at T = 25 °C and below.[37]

obtain,[50] but one possible approach is to determine if the different structures formed by water molecules moving inside the pore possess distinct dependencies on temperature. Our pores are especially suitable for this type of investigation, as they both contain the same amount of water confined to varying extents depending on the pore diameter. This makes it possible to compare the respective stability (upon changing temperature) of the structures formed by the inner water in each system, without having to consider additional variables.

Experimental Methods

Compounds (±)**1**·2H_2O and (±)**2**·2H_2O were synthesized following the synthetic sequence reported for other members of this family of compounds.[31] Suitable crystals of both compounds were grown at room temperature from a damp mixture of carbon tetrachloride/2,2,4-trimethylpentane (4:1).

Thermogravimetric analysis was performed with a Mettler TGA/sDTA851e analyzer, under a mixture of dry air and nitrogen. The amount of material used in the TGA studies ranged from approximately 4.6 mg to 7.5 mg. The temperature was typically increased at a heating rate of 1 deg/min. Additionally, we ran experiments where the samples were heated, held at certain temperatures for some time and then heated again. DSC experiments were previously reported for both samples.[36]

A Bruker D8 with an Anton Parr high-temperature platinum stage was used for the variable-temperature X-ray diffraction (VT-PXRD) experiments. Two series of experiments were performed. In the first one, each sample was continuously heated from 30 to 180 °C at a heating rate of 1 deg/min, with XRD patterns recorded every 5 °C. A 2θ range of 5° to 70° was used, with steps of 0.025° and 28.8 s per step as acquisition time. The second series involved holding the samples at certain temperatures and recording successive diffraction patterns to monitor eventual changes. The total temperature range for both samples was 30 to 150 °C, at a heating rate of 1 deg/min. The following parameters were used for acquisition of the diffraction data: a 2θ range from 5° to 50°, steps of 0.025° or 0.028°, and 28.8 s per step. Both series were run under air. Approximately 10 mg of material was typically used for each measurement. The organic sample was dispersed with acetone to make a slurry, which was then pasted on the sample stage. The measurements were carried out after the mixture was dry. Because of the small sample size the data collection was carried out in short steps with long acquisition times.

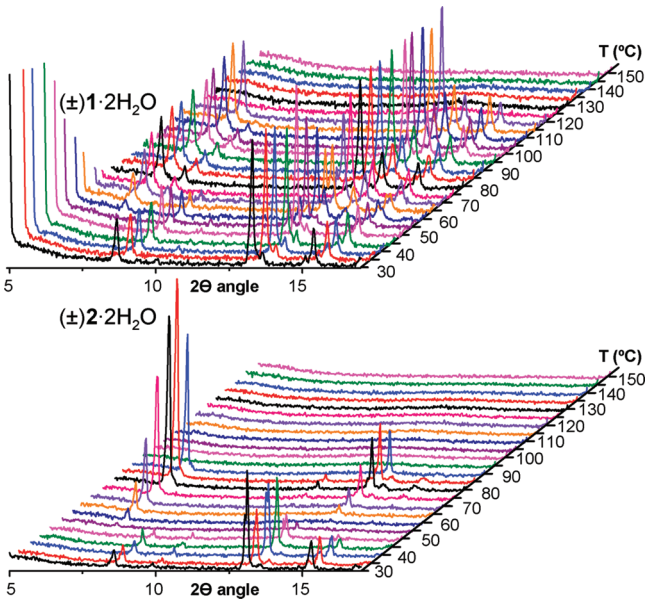

Figure 3. VT-PXRD diffraction patterns for (±)**1**·2H_2O (up) and (±)**2**·2H_2O (down) obtained by increasing the temperature from 30 °C to150 at 1 deg/min.

Results and Discussion

Parallel thermogravimetric analysis (TGA) as well as variable-temperature powder X-ray diffraction measurements (VT-PXRD) were performed on crystalline samples of (±)**1**·2H_2O (which forms the wider pores) and (±)**2**·2H_2O (which forms narrower pores) in order to monitor both dehydration events and structural phase transitions upon increasing temperature of the porous structures.

In the first series of VT-XRD experiments, the temperature was increased at 1 deg/min from 30 to 150 °C and diffraction patterns were recorded every 5 min. The results clearly indicate that the solids remain crystalline up to about 100 °C (Figure 3). Under these conditions a phase transition was observed as the temperature of the hydrated form of (±)**1**·2H_2O reached about 65 −70 °C. This phase remained stable up to a temperature of approximately 120 °C, after which the sample decomposes. VT-PXRD analysis of the observed peak positions of the sample of (±)**2**·2H_2O, which has a smaller inner diameter, showed that an analogous phase transition occurs at lower temperature, namely between 50 and 55 °C. In this case the resulting structure is stable until approximately 90 °C. This phase transition in both systems most likely corresponds to a reorganization of the organic molecules forming the supramolecular structure, which induces irreversible changes in size and shape.

The dehydration for these two structures was also studied in parallel by thermogravimetric analysis (TGA) at a scan rate of 1 deg/min (Figure 4).

The loss of water from (±)**1**·2H_2O occurred in two well-defined events: first, between approximately 28 and 48 °C and immediately afterward between approximately 50 and 85 °C. The weight losses associated with each event were 4.3% and 8.0%, respectively, in agreement with the theoretical value of 12.9% weight which corresponds to the total water content in the sample.

The TGA results for (±)**1**·2H_2O in conjunction with the VT-PXRD data described above lead to the following assertions: The starting porous self-assembly clearly is stable even after a certain degree of dehydration. After the phase transition

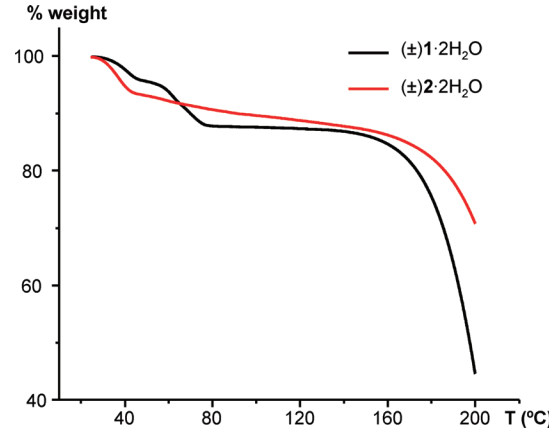

Figure 4. TGA curves for (±)**1**·2H_2O (black line) and (±)**2**·2H_2O (red line) obtained with a heating rate of 1 deg/min.

observed by VT-PXRD, the sample does also persist in losing water, which in turn points to the formation of an anhydrous phase.

Analysis of the TGA results for (±)**2**·2H_2O also reveals an initial dehydration step between approximately 28 and 54 °C, which accounts for a weight loss of 6.9%. Subsequently water is gradually lost in a second, much smoother event, which did not reach a real plateau as the sample started to decompose in the same range of temperatures. A weight loss of 4.4% was measured between 55 °C and approximately 125 °C. The sum of both values agrees well with the theoretical water content of 11.9%. Consideration of these TGA analyses along with the VT-PXRD data leads to a similar description of the events in this system. As for the previous case the initial hydrated structure remains stable after some degree of dehydration. In this sample, however, it is not clear that the phase transition results in a completely anhydrous structure as it appears to collapse at around 90 °C, before water is totally removed.

These initial results prompted us to redesign our experiment in a way to answer the following questions: Is it possible to keep the initial porous structure intact after partial or even total dehydration despite the fact that this structure is the result of the incorporation of water in the self-assembling process? Do both samples release water with the same ease? Is it possible to release a certain amount of water and rehydrate the samples after a proper treatment? Since the first phase transition and final decomposition of these samples was observed upon heating of the samples at a uniform rate, our following TGA and VT-PXRD measurements were performed on both samples by keeping the temperatures fixed at specific points a certain time rather than steadily increasing the temperature.

TGA measurements on (±)**1**·2H_2O were performed with a uniform heating rate of 1 deg/min except that the temperature was kept constant at 40 °C and again at 65 °C 30 min each. We used the same heating rate for (±)**2**·2H_2O and in this case the temperature was kept fixed at 35 and 45 °C for 30 min each (Figure 5). In both samples, the first temperature that was held constant for 30 min corresponds to the initial porous structure, and under these conditions it is observed that approximately half of the water present in (±)**1**·2H_2O and approximately two-thirds of the water present in (±)**2**·2H_2O could readily be evacuated at this constant temperature.

The dehydration in (±)**1**·2H_2O corresponds to the VT-PXRD pattern shown in Figure 3 (top), where the two consecutive steps occurred at slightly lower temperatures. In contrast, the weight loss in (±)**2**·2H_2O does not occur in discrete steps but rather

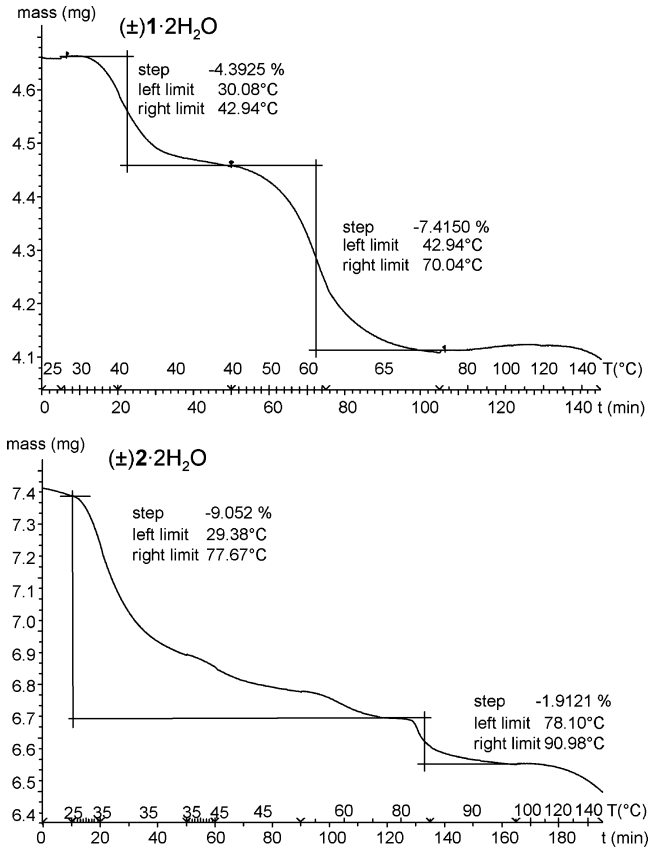

Figure 5. TGA curves obtained for 4.66 mg of (±)**1**·2H_2O (top) and 7.41 mg of (±)**2**·2H_2O (bottom) showing the release of water when the temperature is maintained fixed at certain values. The upper part of the *x*-axis represents the temperature, and the bottom part represents the time. The water loss is indicated by the step function above the curve. The theoretical values for a 100% of water loss is 12.95% of mass in the case of compound (±)**1**·2H_2O and 11.92% of mass in the case of compound (±)**2**·2H_2O. For the particular masses employed in this experiment, these values correspond with a "dry weight" of 4.06 mg in the case of compound (±)**1**·2H_2O and 6.53 mg in the case of compound (±)**2**·2H_2O.

in a gradual way such that the largest loss takes place between 25 and 35 °C, but then the system needs to reach a temperature greater than 90 °C for complete dehydration. These results again point to the fact that the initial porous structure is maintained even after the majority of the water molecules are released from it.

To check the observation that compound (±)**2**·2H_2O released a large percentage of water close to room temperature, a following TGA experiment for this sample was carried out with the temperature kept constant at 30 °C for 2 h before raising it at a rate of 1 deg/min (Figure 6).

Under these very smooth conditions, the (±)**2**·2H_2O sample releases more than 80% of its water content. Complete dehydration, however, again is not achieved until the temperature reaches nearly 100 °C. In the case of (±)**1**·2H_2O, on the other hand, complete dehydration took place at about 65 °C (Figure 5), which coincides with the temperature of the phase transition determined by VT-PXRD (Figure 3). The difference in the dehydration temperature ($\Delta T \approx 30$ °C) of the two types of pores can clearly be attributable to the stronger interactions between the pore surface and the adsorbed water for the pore with the smaller diameter (i.e., the one formed by the monomer **2**).

The TGA experiments just described do not, however, match the heating profiles of the first set of VT-XRD experiments.

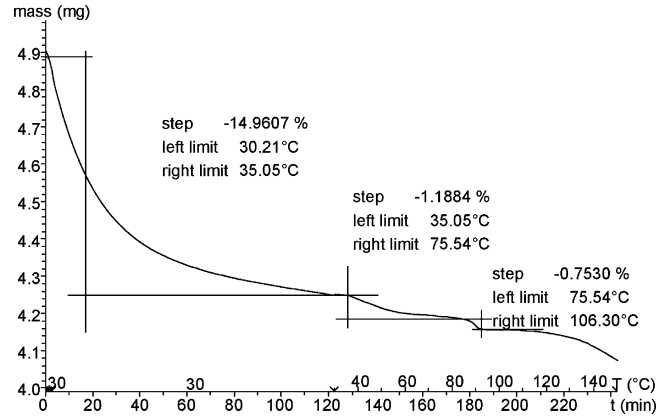

Figure 6. TGA curve obtained for 4.90 mg of (±)**2**·2H_2O showing the smooth release of water (~80% of the total content) when the temperature was maintained at 30 °C for 2 h. The upper part of the *x*-axis represents the temperature, and the bottom part represents the time. The water loss is indicated by the step function above the curve. The theoretical values for a 100% of water loss is 11.92% of mass in the case of compound (±)**2**·2H_2O. This value corresponds with a "dry weight" of 4.32 mg in this sample.

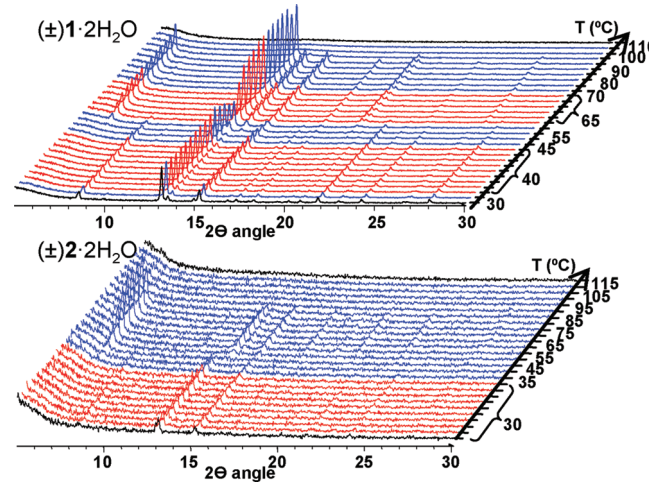

Figure 7. VT-PXRD diffraction patterns for (±)**1**·2H_2O (up) and (±)**2**·2H_2O (down) obtained by increasing the temperature from 30 to 150 °C: black, initial and final scans at 30 and 150 °C, respectively; blue, scans obtained in 5 deg intervals with increasing temperature (heating rate = 1 deg/min); red, data obtained at constant temperatures of 40 and 65 °C (a) and 30 °C (b).

We therefore carried out a second set of VT-PXRD measurements so that we could verify the expected crystal structures at each temperature and at the same time study the possible influence of the gradual dehydration on the phase transitions. This was accomplished by keeping the sample temperature constant at certain points for a given time on both (±)**1**·2H_2O and (±)**2**·2H_2O (Figure 7). The same conditions as in the TGA experiments where chosen: in the case of (±)**1**·2H_2O, temperature was kept constant at 40 and 65 °C and increased at 1 deg/min for the rest of the scan (comparable to Figure 5a) and in the case of (±)**2**·2H_2O the temperature was kept constant at 30 °C for 2 h (comparable to Figure 6) and increased at 1 deg/min for the rest of the scan.

The phase transitions in both samples occurred in the same temperature ranges as before, although the ultimate collapse of the crystal structure occurred at slightly lower temperatures. These results unambiguously lead to two important conclusions: the phase transitions are largely independent of the amount of water present in the pore at any particular time and independent

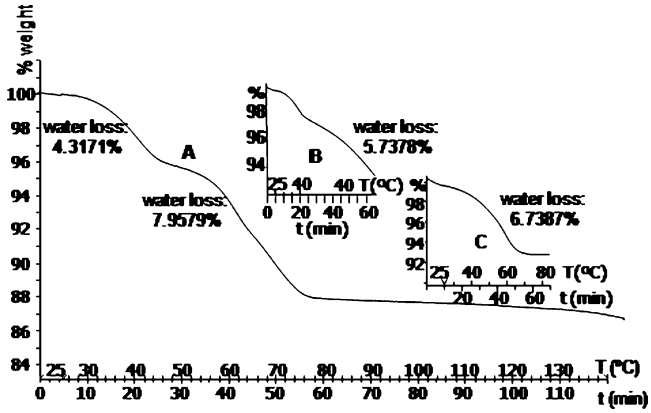

Figure 8. Three superimposed TGA experiments on the pore formed by (±)**1**·2H_2O: (A) "continuous" experiment (same plot as in Figure 4); (B) "partial dehydration" experiment; and (C) "rehydration" experiment, after the sample used for part B was kept 24 h under a humid atmosphere. Water loss percentages in each step are also depicted.

of the temperature ramp used, and as a consequence of this, the initial structure is stable even up to the point of nearly complete dehydration. This can be seen particularly clearly in the case of (±)**2**·2H_2O in the last series of experiments. Single-crystal X-ray diffraction results of a crystal of this compound, which was previously heated to 40 °C for several hours, showed that the initial crystalline phase indeed remains intact.

A crucial finding from these experiments is that the intrinsic structure of both crystals with different pores was retained during the partial dehydration process. This result implies that the internal characteristics of the pore surfaces remain unaltered so that it is possible to study the temperature-induced effect on the hydration−dehydration phenomenon independently. While approximately about one-half of the water molecules present in the pore with the larger diameter, (±)**1**·2H_2O, could be evacuated when the temperature was kept fixed at 40 °C during 40 min (see Figure 8, plot B), rehydration unexpectedly did not occur when the partially dehydrated sample was maintained at room temperature under a humid atmosphere for 24 h before increasing the temperature to 80 °C in a new TGA experiment (Figure 8, plot C).

This observation indicates that the cooperative behavior of confined water molecules is central to the hydration process, and their absence renders the system essentially hydrophobic. These findings not only highlight the differing roles played by the two types of water molecules present in the pore, but also point to the need for a presence of freely moving water molecules inside the pore to sustain its permeability by water. Finally, our results open the door to a comprehensive experimental exploration of model systems where the qualitative physical-chemical principles that make water so special in the function of biological processes[51] can be systematically studied and de novo design models benchmarked.

Conclusions

There has been an increasing amount of experimental evidence to support the idea that water molecules can continuously occupy permanently nonpolar pores. In this work we show that hydrophobicity as opposed to hydrophilicity cannot be taken to be an absolute property of a porous surface without taking the structure of the water moving within the pore into account.[52] Under certain conditions, the pore can be dried, which means, in terms of classical thermodynamics, that water does not wet the inner surface of the pore.

The ability to wet the pore surface was found to correlate with the size of the cavity and the strength of the interaction between water molecules and the walls of the cavity,[53] which in turn can be modulated by changes in temperature. The differences in the temperature dependence of dehydration and the phase transitions exhibited by the porous structures, (±)**1**·2H_2O and (±)**2**·2H_2O, leads to the conclusion that the variations of the behavior of water inside the pore depends strongly on the details of the interatomic interactions between water molecules and with the interior surface of the pore. The switch in the fluctuating surface wetting ability observed in both model systems suggests that the structure and dynamics of local water are significantly affected by temperature. The hydration−dehydration phenomenon in structurally intact pores appears to result from a sensitive balance between surface water and water−water interaction energies in terms of the enthalpy/entropy compensation principle.[54]

The presence of water near hydrophobic surfaces is common in biological systems and plays a crucial role in various important biophysical phenomena, such as the functional dynamics and thermodynamics of natural pores and the folding and function of proteins. Our results on the fundamental chemical principles of the interactions between water molecules and hydrophobic pores should advance the molecular-level understanding of many of these biological processes. Related research is currently being carried out with the aim to obtain a more detailed understanding of local density fluctuations of water by means of inducing subtle modulations in pore diameter and flexibility.

Acknowledgment. The financial support from the Spanish Ministry of Science and Technology (MST/FEDER) is gratefully acknowledged (project CTQ2007-61024/BQU). This work made use of the Central Facilities of the Materials Research Laboratory supported by the National Science Foundation (DMR05-20415).

References and Notes

(1) Agre, P. *Angew. Chem., Int. Ed.* **2004**, *43*, 4278–4290.
(2) Preston, G. M.; Carroll, T. P.; Guggino, W. B.; Agre, P. *Science* **1992**, *256*, 385–387.
(3) Murata, K.; Mitsuoka, K.; Hirai, T.; Walz, T.; Agre, P.; Heymann, J. B.; Engel, A.; Fujiyoshi, Y. *Nature* **2000**, *407*, 599–605.
(4) Ren, G.; Reddy, V. S.; Cheng, A.; Melnyk, P.; Mitra, A. K. *Proc. Natl. Acad. Sci. U.S.A.* **2001**, *98*, 1398–1403.
(5) De Groot, B. L.; Grubmüller, H. *Science* **2001**, *294*, 2353–2357.
(6) Hummer, G.; Rasaiah, J. C.; Noworyta, J. P. *Nature* **2001**, *414*, 188–190.
(7) Andreev, S.; Reichman, D.; Hummer, G. *J. Chem. Phys.* **2005**, *123*, 194502/1–9.
(8) Cicero, G.; Grossman, J. C.; Schwegler, E.; Gygi, F.; Galli, G. *J. Am. Chem. Soc.* **2008**, *130*, 1871–1878.
(9) O'Connell, M. J. *Carbon Nanotubes: Properties and Applications*; CRC Press: Boca Raton, FL, 2006.
(10) Sui, H.; Han, B. G.; Lee, J. K.; Walian, P.; Jap, B. K. *Nature* **2001**, *414*, 872–878.
(11) Rasaiah, J. C.; Garde, S.; Hummer, G. *Annu. Rev. Phys. Chem.* **2008**, *59*, 713–740.
(12) Zhu, F.; Schulten, K. *Biophys. J.* **2003**, *85*, 236–244.
(13) Fang, H.; Wan, R.; Gong, X.; Lu, H.; Li, S. *J. Phys. D: Appl. Phys.* **2008**, *41*, 1–16.
(14) Kolesnikov, A. I.; Zanotti, J. M.; Loong, C. K.; Thiyagarajan, P.; Moravsky, A. P.; Loutfy, R. O.; Burnham, C. J. *Phys. Rev. Lett.* **2004**, *93*, 035503/1–4.
(15) Chou, C. C.; Hsiao, H. Y.; Hong, Q. S.; Chen, C. H.; Peng, Y. W.; Chen, H. W.; Yang, P. C. *Nano Lett.* **2008**, *8*, 437–445.
(16) Tajkhorshid, E.; Nollert, P.; Jensen, M. O.; Miercke, L. J.; O'Connell, J.; Stroud, R. M.; Schulten, K. *Science* **2002**, *296*, 525–530.
(17) Bianco, A.; Kostarelos, K.; Prato, M. *Curr. Opin. Chem. Biol.* **2005**, *9*, 674–679.
(18) Alexiadis, A.; Kassinos, S. *Chem. Rev.* **2008**, *108*, 5014–5034.
(19) Köfinger, J.; Hummer, G.; Dellago, C. *Proc. Natl. Acad. Sci. U.S.A.* **2008**, *105*, 13218–13222.

(20) Waghe, A.; Rasaiah, J.; Hummer, G. *J. Chem. Phys.* **2002**, *117*, 10789–10795.
(21) Won, C. Y.; Aluru, N. R. *J. Am. Chem. Soc.* **2007**, *129*, 2748–2749.
(22) Nanok, T.; Artrith, N.; Pantu, P.; Bopp, P.; Limtrakul, J. *J. Phys. Chem. A* **2009**, *113*, 2103–2108.
(23) Mashl, R.; Joseph, S.; Aluru, N.; Jakobsson, E. *Nano Lett.* **2003**, *3*, 589–592.
(24) Liu, Y.; Wang, Q.; Wu, T.; Zhang, L. *J. Chem. Phys.* **2005**, *123*, 234701–234707.
(25) Koga, K.; Tanaka, H.; Zeng, X. C. *Nature* **2000**, *408*, 564–567.
(26) Liu, Y; Wang, Q. *Phys. Rev. B* **2005**, *72*, 1–4.
(27) Liu, Y.; Wang, Q.; Zhang, L.; Wu, T. *Langmuir* **2005**, *21*, 12025–12030.
(28) Joseph, S.; Aluru, N. R. *Nano Lett.* **2008**, *8*, 452–458.
(29) Won, C. Y.; Aluru, N. R. *J. Phys. Chem. C* **2008**, *112*, 1812–1818.
(30) Hoffmann, R.; Schleyer, P. v. R.; Schaefer, H. F., III *Angew. Chem., Int. Ed.* **2008**, *47*, 7164–7167.
(31) In all cases, the solid state structures of the crystalline materials were investigated by X-ray diffraction on single crystals: Carrasco, H.; Foces-Foces, C.; Pérez, C.; Rodríguez, M. L.; Martín, J. D. *J. Am. Chem. Soc.* **2001**, *123*, 11970–11981.
(32) Pérez, C.; Espínola, C. G.; Foces-Foces, C.; Núñez-Coello, P.; Carrasco, H.; Martín, J. D. *Org. Lett.* **2000**, *2*, 1185–1188.
(33) Pérez, C.; Rodríguez, M. L.; Foces-Foces, C.; Pérez-Hernández, N.; Pérez, R.; Martín, J. D. *Org. Lett.* **2003**, *5*, 641–644.
(34) Febles, M.; Pérez, C.; Foces-Foces, C.; Rodríguez, M. L.; Pérez-Hernández, N.; Morales, E. Q.; Martín, J. D. *Org. Lett.* **2004**, *6*, 877–880.
(35) Pérez-Hernández, N.; Roux, M. V.; Febles, M.; Morales, E. Q.; Pérez, C.; Fort, D.; Martín, J. D. *Z. Phys. Chem.* **2008**, *322*, 1477–1478.
(36) Febles, M.; Pérez-Hernández, N.; Pérez, C.; Rodríguez, M. L.; Foces-Foces, C.; Roux, M. V.; Morales, E. Q.; Buntkowsky, G.; Limbach, H. H.; Martín, J. D. *J. Am. Chem. Soc.* **2006**, *128*, 10008–10009.
(37) Beckstein, O.; Sansom, M. S. *Proc. Natl. Acad. Sci. U.S.A.* **2003**, *100*, 7063–7068.
(38) Yu, B.; Blaber, M.; Gronenborn, A. M.; Clore, G. M.; Caspar, D. L. *Proc. Natl. Acad. Sci. U.S.A.* **1999**, *96*, 103–108.
(39) Buckle, A. M.; Cramer, P.; Fersht, A. R. *Biochemistry* **1996**, 4298–4305.
(40) Liu, K.; Cruzan, J. D.; Saykally, R. J. *Science* **1996**, *271*, 929–933.
(41) Liu, K.; Brown, M. G.; Carter, C.; Saykally, R. J. *Nature* **1996**, *381*, 501–503.
(42) Cruzan, J. D.; Braly, L. B.; Liu, K.; Brown, M. G.; Loeser, J. G.; Saykally, R. J. *Science* **1996**, *271*, 59–62.
(43) Liu, K.; Brown, M. G.; Cruzan, J. D.; Saykally, R. J. *Science* **1996**, *271*, 62–64.
(44) Gruenloh, C. J.; Carney, J. R.; Arrington, C. A.; Zwier, T. S.; Freedericks, S. Y.; Jordan, K. D. *Science* **1997**, *276*, 1678–1681.
(45) Kim, J.; Kim, K. S. *J. Chem. Phys.* **1998**, *109*, 5886–5895.
(46) Keutsch, F. N.; Saykally, R. J. *Proc. Natl. Acad. Sci. U.S.A.* **2001**, *98*, 10533–10540.
(47) Nauta, K.; Miller, R. E. *Science* **2000**, *287*, 293–295.
(48) Granick, S.; Bae, S.-Ch. *Science* **2008**, *322*, 1477–1478.
(49) Wang, H.-J.; Xi, X.-K.; Kleinhammes, A.; Wu, Y. *Science* **2008**, *322*, 80–83.
(50) Chandler, D. *Nature* **2005**, *437*, 640–647.
(51) Ohba, T.; Kanoh, H.; Kaneko, K. *Chem.—Eur. J.* **2005**, *11*, 4890–4894.
(52) Ball, P. *Chem. Rev.* **2008**, *108*, 74–108.
(53) Vaitheeswaran, S.; Yin, H.; Rasaiah, J. C.; Hummer, G. *Proc. Natl. Acad. Sci. U.S.A.* **2004**, *101*, 17002–17005.
(54) Fisicaro, E.; Compari, C.; Braibanti, A. *Phys. Chem. Chem. Phys.* **2004**, 4156–4166.

JP911930K